

Nature and Stability of Weak Halogen Bonds in the Gas Phase: Molecular Beam Scattering Experiments and Ab Initio Charge Displacement Calculations

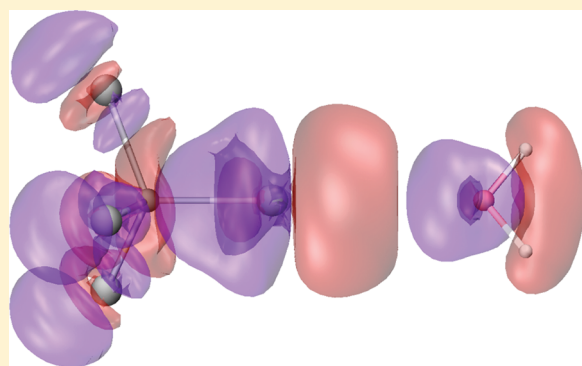
Published as part of the *Crystal Growth & Design* virtual special issue on *Halogen Bonding in Crystal Engineering: Fundamentals and Applications*

David Cappelletti,^{*,†} Pietro Candori,[†] Fernando Pirani,[‡] Leonardo Belpassi,^{‡,§} and Francesco Tarantelli^{‡,§}

[†]Dipartimento di Ingegneria Civile ed Ambientale and [‡]Dipartimento di Chimica, Università degli Studi di Perugia, Perugia, Italy

[§]CNR - Istituto di Scienze e Tecnologie Molecolari, Perugia, Italy

ABSTRACT: Molecular beam scattering experiments are presented for the first time in order to characterize the nature and strength of the intermolecular interaction of the gas phase $\text{H}_2\text{O}-\text{CF}_4$ and $\text{H}_2\text{O}-\text{CCl}_4$ weakly bound complexes. Simultaneous measurements of the collision cross section of water, molecular oxygen, and argon atoms scattered by the same target (CF_4 or CCl_4) have been performed in the thermal energy range. The experimental results show unambiguously that $\text{H}_2\text{O}-\text{CCl}_4$ is ~ 0.5 kJ/mol more stable than O_2-CCl_4 and $\text{Ar}-\text{CCl}_4$, which is incompatible with a fully noncovalent nature of the interaction. Interestingly, this is not the case for the analogous CF_4 complexes which all show the same binding energy, within the experimental uncertainty. These results are supported by state-of-the-art ab initio calculation of the dimer structures and of the charge displacement upon the formation of the complex. The focus is on the possible stabilization effects due to halogen bond formation and on the extent of the related charge transfer. The latter has been shown to be large from H_2O toward CCl_4 and negligible from H_2O toward CF_4 .



Halogen bonding (XB), despite a long history dating back more than one century,¹ marked by classic highlights such as those of Mulliken² and Hassel,³ has been a relatively unexplored interaction until about two decades ago, when it started attracting a lot of attention.⁴ Specifically, the high directionality and the strength of XB, which may range between 5 and 180 kJ mol⁻¹, are of great relevance in molecular recognition processes and crystal packing.^{5,6} For these reasons, XB has already found applications in a wide range of fields which include crystal engineering, superconductors, liquid crystals, nanoparticles, and drug design. This has also driven renewed efforts in the investigation of its nature.⁴

Briefly, the early view of XB origin was basically based on a charge-transfer (CT) model of the interaction, authoritatively put forward by Mulliken.² This had an effect also on the commonly accepted terminology: indeed, definitions still widely in use today for XB such as *electron donor and acceptor* and *halogen atom donor and acceptor*, imply, at least conceptually, some degree of CT or covalency. Lately, with the improvement of experimental techniques and theoretical tools, more complex landscapes appeared for intermolecular forces, and also other components of the interaction (electrostatic, dispersion and induction) have been shown to play a relevant role.^{7–10} For

some classes of compounds, such as, for instance, those involving halogen molecules, the charge exchange with electron donor counterparts is dominating the interaction.^{1,11} For other compounds, such as the $\text{R}-\text{X}$ molecules where R is an electron withdrawing group (e.g., CF_3Br), electrostatic contributions arising from anisotropic electronic charge distributions are relevant and dictate the geometries of the formed complexes.^{1,9}

The straightforward perspective that models based on electrostatic properties of the isolated fragments can provide for the properties of the formed complex is noteworthy: actually one of our main efforts in the modeling of intermolecular interactions has been the proposal of correlation formulas between the basic properties of isolated species (electronic polarizability,¹² permanent multipole moments and charges^{13,14}) and the main intermolecular interaction parameters for noncovalently bound systems. Among them, the weakly interacting neutral–neutral complexes are often identified as van-der-Waals (vdW) systems. In the present paper, we shall exploit the predictive power of such semiempirical analysis for the study of XB. At a deeper look, and when not only the geometric structure but also the stabilization

Received: July 13, 2011

Published: August 18, 2011

energy is considered, it emerges clearly that, in many cases, intermolecular interactions arise from a delicate balance of several and often not fully separable interaction components. This is evident, for example, when one examines the behavior of experimental signatures of XB, such as the shift of spectral lines (red or blue) that often, as in the case of hydrogen bonding (HB), are difficult to rationalize within too simple models.^{15–17} Another example is the case of the $\text{H}_2\text{O}-\text{X}_2$ systems, which are well-known¹⁸ and to some extent related to the presently studied cases. For these dimers, stable halogen bond configurations are generally found (also for fluorine), and for the mixed $\text{H}_2\text{O}-\text{ClF}$ complex an electron donation is apparent toward the Cl end of the halogen molecule.¹⁹

In extreme synthesis, the current view of XB^{1,5,11,20,21} is that many interaction components (CT, electrostatic, dispersion, induction, ...) are present, but they may play a very different role from system to system. Indeed, the HB acceptor capabilities of the halogens,²² competition between HB and XB,^{23,24} and the combination of XB with other interactions (such as, for instance, aurophilic interactions²⁵) are all issues of great interest and represent complementary aspects of a complex phenomenology.

The parallelism between XB and HB⁵ is one of the themes that motivated the present work. Recently, we have developed an integrated experimental and theoretical approach to reveal CT effects in weak intermolecular HB.^{26–29} Here we are trying to add some pieces to the XB mosaic along the same lines. Specifically, we have chosen to compare the gas phase behavior of $\text{H}_2\text{O}-\text{CF}_4$ and $\text{H}_2\text{O}-\text{CCl}_4$. Gas phase studies, in particular those exploiting molecular beams, are ideal because environmental effects are absent and a direct comparison with computed structure is possible.³⁰ For the above systems, electrostatic effects may be expected to play a minor role due to the high symmetry of the CF_4 and CCl_4 molecules. Moreover, a competition of HB with XB is expected, at least for some configurations of their complexes with water. We shall thus present new experimental findings for these complexes and a theoretical analysis of their XB configurations. A more complete study, including the characterization of HB, is ongoing and will be presented soon.

Not much is available in the literature on the $\text{H}_2\text{O}-\text{CF}_4$ and $\text{H}_2\text{O}-\text{CCl}_4$ systems, especially on the experimental side. Caminati et al.³¹ investigated the rotational spectra of all the $\text{H}_2\text{O}-\text{CF}_4$ isotopologues, finding a stable structure with the oxygen atom facing the CF_3 group along a C_3 symmetry axis (the *face* configuration). High level ab initio calculations are also available³² for the $\text{H}_2\text{O}-\text{CF}_4$ dimer, which are in essential agreement with the measurements.³¹ To our knowledge, there are no gas-phase experiments on the $\text{H}_2\text{O}-\text{CCl}_4$ dimer, and very little information is available from the theoretical point of view,³³ which suggests a XB stable structure with the O atom pointing toward a C–Cl bond (the *vertex* configuration).

We first tackled the problem through molecular beam scattering experiments aimed at measuring the “glory” quantum interference shift, recently introduced²⁷ as a phenomenological tool to quantify the stabilization by CT in weakly bound intermolecular complexes. As in previous investigations,^{26–29,34} the “glory” shift is evaluated by comparing measurements carried out, under the same experimental conditions, on water, O_2 , or Ar scattered by the same target. This approach is suggested by the semiempirical analysis mentioned above^{12,35} which, based on their very similar polarizabilities, predicts the same vdW component for the interaction of Ar, O_2 , or H_2O with the same counterpart. Indeed, Ar and O_2 behave always similarly when scattered by the same target,

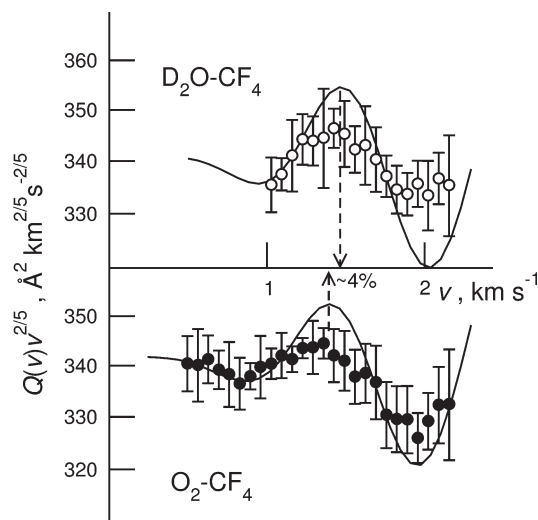


Figure 1. Cross sections Q for the $\text{D}_2\text{O}-\text{CF}_4$ and O_2-CF_4 systems, plotted as function of the beam velocity v . Symbols are the experimental data and lines are the fits using the ILJ potential model (see text, Table 1 and Figure 3). Arrows guide the eye to the glory extrema positions, indicating a glory shift of $\approx 4\%$.

and their experimental data serve as reference for other noncovalent interactions: any deviation of water from them is considered a manifestation of CT stabilization.^{26–29} We note that, in the XB context, the absence of charge exchange for halogens interacting with Ar is well established.¹ Accompanying the experiment, a thorough theoretical analysis of the CT nature of the stabilization contribution is pursued by high level ab initio calculations of the charge displacement in the intermolecular frame.²⁶

The molecular beam (MB) apparatus used in the present experiments has been described in detail elsewhere.³⁶ Briefly, it consists of five differentially pumped vacuum chambers connected by slits for molecular beam collimation. The MB, either D_2O or O_2 , emerges through a heated nozzle (1 mm in diameter, $T_{\text{nozzle}} \sim 500$ K) from an effusive source and is mechanically velocity selected.^{37,38} It then crosses a scattering chamber, which can be filled up with the target gas (CF_4 or CCl_4) by an automated procedure. The chamber is maintained at room temperature ($T_{\text{scat}} = 300$ K). The high rotational temperature conditions of both projectile and target molecules are necessary to avoid cluster formation and quenching effects due to the anisotropy of the interaction. In these conditions, the experimental integral cross sections data are sensitive directly and dominantly to the spherical (isotropic) average of the intermolecular potential energy surface and are determined essentially by elastic collisions, as amply demonstrated in previous work.^{34,36,39–41} The online MB intensity is detected, after the scattering region, by an electron bombardment ionizer followed by a quadrupole mass spectrometer and an electron multiplier. The total integral cross section $Q(v)$ as a function of the selected velocity v of the projectile is obtained by measuring the beam intensities with the target gas in the scattering chamber and without the target gas. Results are plotted in Figure 1 for the O_2-CF_4 and $\text{H}_2\text{O}-\text{CF}_4$ systems and in Figure 2 for the O_2-CCl_4 and $\text{H}_2\text{O}-\text{CCl}_4$ complexes.

We note that the measured magnitude of the cross sections and the amplitude of the observed quantum interference effects altogether indicate a negligible role of the electrostatic contributions³⁴ for the present systems. Moreover, scattering experiments have been performed also for the $\text{Ar}-\text{CCl}_4$ system, but the cross section

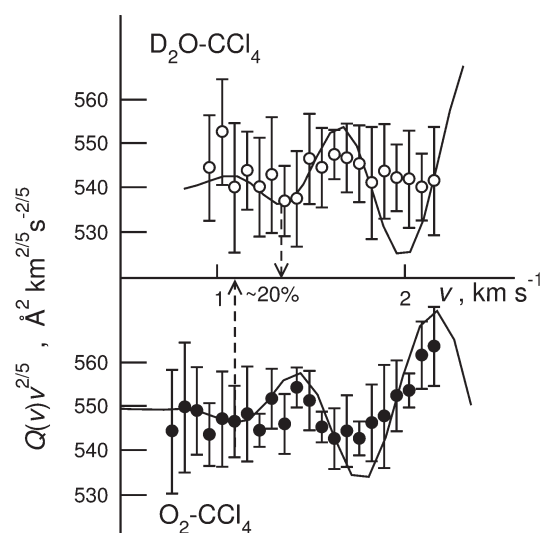


Figure 2. As in Figure 1 but for the $\text{D}_2\text{O}-\text{CCl}_4$ and O_2-CCl_4 systems. The estimated glory shift is $\approx 20\%$.

is not reported in the figure because it is identical, within the experimental uncertainty, to that of O_2-CCl_4 .

$Q(v)$ is one of the few experimental observables (together with the second virial coefficients) directly sensitive to the absolute scale of the interaction. In particular, the position of the glory extrema directly depends on the area of the potential well and is sensitive to its depth, while the magnitude of the cross section is related to the long-range part of the interaction.

In fitting of the experimental data, we used the Improved Lennard-Jones (ILJ) two body model potential,⁴² which is best suited for the description of the present isotropically averaged data. This simple two-parameter model gives also the correct asymptotic behavior of the interaction energy. The cross sections $Q(v)$, calculated in the center of mass frame using the Jeffrey-Wentzel-Kramer-Brillouin (JWKB) method, are convoluted in the laboratory system for direct comparison with the experimental data. The convolution includes the average over the thermal motion of the target gas, the transmission function of the velocity selector, and a small correction to $Q(v)$ due to the finite angular resolution of the apparatus.³⁶

The direct comparison of the O_2 (lower panel) and H_2O (upper panel) experimental data as reported in Figures 1 and 2 show, first of all, that the magnitude of $Q(v)$ is the same, within the experimental uncertainty. This is expected and indicates that the intermolecular potential energy of O_2-CX_4 and $\text{H}_2\text{O}-\text{CX}_4$ at long-range is very similar. Second, for the case of CF_4 , there is a small but measurable glory shift ($\sim 4\%$), while for the $\text{H}_2\text{O}-\text{CCl}_4$ system the shift is much larger (20% or $\sim 200 \text{ m/s}$).

The ϵ and r_m parameters characterizing the ILJ potential obtained here for the water- CX_4 and oxygen- CX_4 systems are reported in Table 1. The same table also reports the values predicted by the semiempirical correlation formula,^{12,35} which take into account the polarizabilities of H_2O , O_2 , and CX_4 and the effects due to the permanent dipole of H_2O . As is evident in Table 1, the glory shift of the $\text{H}_2\text{O}-\text{CCl}_4$ is associated with a net stabilization energy ($\sim 0.5 \text{ kJ/mol}$) compared to the O_2-CCl_4 (vdW) dimer. This is similar to, in fact larger than, the bond stabilization observed ($\sim 0.2 \text{ kJ/mol}$) for the hydrogen-bonded $\text{H}_2\text{O}-\text{H}_2$ system with respect to the vdW bonded O_2-H_2 , where CT was demonstrated to be the cause of stabilization of the bond.²⁸

Table 1. Isotropic Well Depth ϵ (kJ/mol) and Equilibrium Distance r_m (Å) for Argon, Water, and Oxygen Interacting with CF_4 and CCl_4 ^a

system	experimental		predictions	
	ϵ	r_m	ϵ	r_m
$\text{H}_2\text{O}-\text{CF}_4$	1.50	3.92	1.54	3.90
O_2-CF_4	1.40	3.96	1.54	3.96
$\text{Ar}-\text{CF}_4$			1.52	3.96
$\text{H}_2\text{O}-\text{CCl}_4$	2.46	4.40	2.14	4.49
O_2-CCl_4	2.00	4.60	2.16	4.54
$\text{Ar}-\text{CCl}_4$	2.00	4.60	2.15	4.54

^a Predictions of correlations formulas^{12,35} are also reported for comparison. The uncertainties on ϵ and r_m are $\sim 5\%$ and 2% for the experimental data and 10% and 3% for predictions, respectively.

In order to put on a firmer theoretical ground the above phenomenological analysis, we performed extensive quantum chemical calculations addressed to a characterization of the potential energy surface (PES) and then to a detailed analysis of the electronic density of the $\text{H}_2\text{O}-\text{CX}_4$ complexes. In particular, we adopted the charge-displacement (CD) analysis consisting in the partial progressive integration along a specified direction z of the change in electron density $\Delta\rho$ occurring upon formation of the complex. This yields

$$\Delta q(z) = \int_{-\infty}^{\infty} dx \int_{-\infty}^{\infty} dy \int_{-\infty}^z \Delta\rho(x, y, z') dz' \quad (1)$$

Clearly, $\Delta q(z)$ measures, at each point z along the axis, the electron charge that, upon formation of the adduct, is transferred from the right to the left side of the perpendicular plane through z .²⁶ This procedure provides extremely insightful information, in that it gives an exact snapshot of the local charge displacement across the entire molecular framework while, at the same time, freeing the results of the arbitrariness inherent in any charge decomposition model. As a result, we can unambiguously appraise the whole spatial extent and chemical relevance of charge fluctuation and transfer phenomena. The calculations of interaction energies and the electronic density have been carried out at the second-order perturbation theory level (MP2) using the triple- ζ augmented correlation consistent polarized valence basis set (aug-cc-pVTZ)^{43–45} as implemented in the program MOLPRO.⁴⁶ With the basis set used, the CD curves are expected to be well converged.²⁶

Since the main focus of this communication is on XB, most of the results presented here refer to the XB coordinate for both systems. The latter corresponds to water approaching CX_4 with its C_2 axis collinear to a C_3 axis of the halogenide, and with oxygen and a X atom facing each other (the *vertex* geometry). A more complete presentation of the whole PES features will be part of a forthcoming paper. Both CX_4 and water have been taken as rigid-rotors. In this arrangement, the rotation of water about the XB (z) coordinate is essentially free, and for definiteness we consider the orientation where water lies on a CX_4 symmetry plane. The structures of the CX_4 molecules have been obtained by a geometrical optimization at the same theoretical level, obtaining 1.32 and 1.77 Å for the C–F and C–Cl bond lengths, respectively. Water's geometry has been fixed at that corresponding to the average of the ground vibrational states of the isolated molecule, as suggested in ref 47.

In the arrangements described, we found equilibrium F–O and Cl–O distances of 3.23 and 3.01 Å for $\text{H}_2\text{O}-\text{CF}_4$ and $\text{H}_2\text{O}-\text{CCl}_4$, respectively. The corresponding interaction energies, corrected for the basis set superposition error (BSSE) evaluated using the counterpoise correction of Boys and Bernardi,⁴⁸ are 0.7 and 7.8 kJ/mol, respectively. Clearly, the XB configuration is very nearly unstable for the $\text{H}_2\text{O}-\text{CF}_4$ complex. For comparison, we found the absolute minimum, for the *face* configuration (with O pointing toward the CF_3 group), having an interaction energy of about 4.3 kJ/mol, which is in good agreement with both previous theoretical³² and experimental³¹ results.

At variance with $\text{H}_2\text{O}-\text{CF}_4$, the (vertex) XB configuration is the most stable in the $\text{H}_2\text{O}-\text{CCl}_4$ case. For this complex, the *face* configuration presents an interaction energy about 4 kJ/mol smaller than the XB one. Other stable configurations are found but at least 2 kJ/mol above the XB one.

The CD curve analysis casts new strong light on these findings. Let us start with the $\text{H}_2\text{O}-\text{CF}_4$ complex. The lower panel in Figure 3 shows isosurfaces of the electronic density difference. The upper panel displays, on the same horizontal scale, the CD curve defined earlier. The dotted vertical red line marks a boundary between the noninteracting fragments, determined by the intersection of equal, tangent isodensity levels of the isolated fragments with the z axis. The density deformation isosurface shows that the CF_4 electron cloud is polarized by the presence of water. This polarization is essentially oriented in the direction of the water's dipole. A large density depletion lobe at the F site pointing toward oxygen extends toward the water molecule. It is evident that the density deformation forms a sort of regular pattern, along the z axis, in which zones of density depletion alternate with zones of density accumulations. By contrast, almost negligible charge rearrangement affects the water molecule: only a small density accumulation is visible at the oxygen site, toward CF_4 . The analysis of the corresponding Δq curve gives a quantitative picture of the interaction and suggests no net CT for this complex. In the whole region of the water molecule, the curve is flat and very close to zero. The curve crosses zero in the region between the fragments, at about 0.17 Å from oxygen. Remarkably, this point practically coincides with the isodensity boundary. It is interesting to note that the curve from this negligible value of the isodensity reaches rapidly a value of 9.9 me at the site of the fluoride atom pointing the water. This reflects, and actually measures, the extent of charge depletion observed above. The pattern displayed by the Δq curve for this system strongly resembles that of a typical vdW complex.²⁶

The result of our analysis for the $\text{H}_2\text{O}-\text{CCl}_4$ in the analogous XB configuration is reported in Figure 4 and reveals immediately a remarkably different pattern. The isosurface of the density deformation, in this case, indicates that the density fluctuations are much more pronounced. Note that the depletion lobe at the chlorine pointing toward oxygen extends in the region between the fragments and appreciably crosses their isodensity boundary. What is further eye-catching is the very pronounced charge rearrangement taking place at the water site, in contrast again with the water– CF_4 case. There is a clear charge accumulation at the oxygen accompanied by a corresponding decrease at the hydrogens. The $\Delta q(z)$ curve quantifies in detail these differences between the two complexes and, above all, shows immediately an important qualitative signature: it is distinctly positive everywhere over the whole complex, never approaching zero. This is the most clear evidence of a net CT from water to CCl_4 .

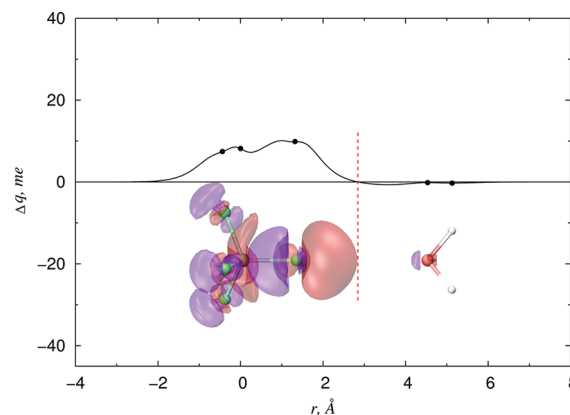


Figure 3. CD curve Δq and 3D isosurface of the electronic density difference accompanying the formation of the $\text{H}_2\text{O}-\text{CF}_4$ complex along the XB coordinate (see text). The red isosurface denotes a negative values of -0.15 me/bohr^3 (density depletion), while the blue one corresponds to a positive value (density accumulation) of 0.15 me/bohr^3 . The red line marks the tangent isodensity boundary of the isolated fragments. The black circles on the CD curve correspond to the projection of the nuclear positions on the integration axis z . The latter is the line joining the centers of mass of the two molecules and has origin at the c.m. of CF_4 .

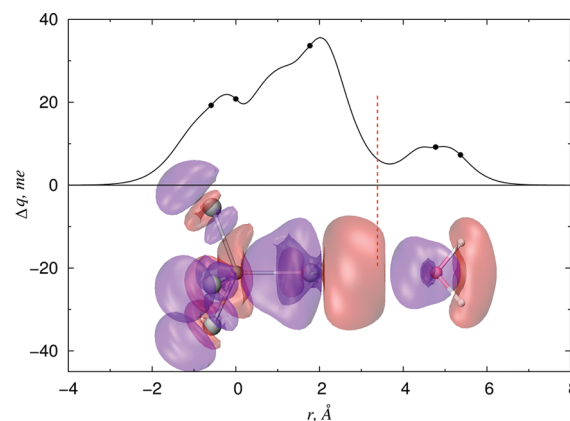


Figure 4. As in Figure 3 but for the $\text{H}_2\text{O}-\text{CCl}_4$ complex.

Electrons start flowing to the left already on the right side of water, so that 7.3 me have moved across the site of the hydrogen atoms. Further to the left, the CD value does not vary much over the whole water region, with a maximum of about 9.2 me near the oxygen site. After this charge starts to reaccumulate and a minimum on the curve is found. The position of a such minimum is close to the isodensity boundary between the fragments, which is at 1.43 Å from the oxygen. At this point the Δq value, which we may take as an estimate of CT from water to CCl_4 , is 6.7 me. For comparison, this is much larger than that computed for the $\text{H}_2\text{O}-\text{H}_2$ complex (2.85 me).²⁸

In conclusion, a net CT from water to CCl_4 in the XB configuration has been revealed by our calculations of the electronic density changes upon complex formation. This CT transfer is not present for the CF_4 case. This evidence is correlated with the experimentally observed stabilization energy of the $\text{H}_2\text{O}-\text{CCl}_4$ complex. We stress that the experimental observable, the “glory” shift, cannot be due to electrostatic or

dispersion terms; therefore, it is a measure of the net effect of CT on the bond strength.

Electrostatic and dispersion contributions are also present in the XB configuration of $\text{H}_2\text{O}-\text{CCl}_4$, which, we underline again, is the most stable one. A preliminary estimate based on semi-empirical calculations^{12,14} and exploiting the CT model developed in ref 28 suggests a similar relative weight of dispersion, charge transfer, and electrostatic contributions to the formation of the bond in $\text{H}_2\text{O}-\text{CCl}_4$. A quantitative comparison between experiment and theory and a complete description of the present systems will require the calculation of CD for a wide range of geometries. This is an ongoing project that will also explore the role of the HB interaction, which most probably plays a role in both the $\text{H}_2\text{O}-\text{CF}_4$ and $\text{H}_2\text{O}-\text{CCl}_4$ dimers at other geometries.

AUTHOR INFORMATION

Corresponding Author

*E-mail: david.cappelletti@unipg.it.

ACKNOWLEDGMENT

This work has been supported by the MIUR PRIN Grant No. 2008KJX4SN_009. PC gratefully acknowledge financial support by Regione Umbria project POR UMBRIA FSE 2007-2013 Asse II "Occupabilità", Obiettivo specifico "e" - Asse IV "Capitale Umano", Obiettivo specifico "I". "Ricerca di Base" n. 2010.011.0501 funded by the Fondazione Cassa di Risparmio Perugia.

REFERENCES

- (1) Legon, A. *Phys. Chem. Chem. Phys.* **2010**, *12*, 7736.
- (2) Mulliken, R. S.; Person, W. B. *Molecular Complexes*; John Wiley & Sons: New York, 1969.
- (3) Hassel, O. *Science* **1970**, *170*, 497.
- (4) *Halogen Bondings: Fundamentals and Applications*; Metrangolo, P.; Resnati, G. Eds.; Springer: Berlin, 2008.
- (5) Metrangolo, P.; Neukirch, H.; Pilati, T.; Resnati, G. *Acc. Chem. Res.* **2005**, *38*, 386.
- (6) Metrangolo, P.; Carcenac, Y.; Lahtinen, M.; Pilati, T.; Rissanen, K.; Vij, A.; Resnati, G. *Science* **2009**, *323*, 1461.
- (7) Lommerse, J.; Stone, A.; Taylor, R.; Allen, F. H. *J. Am. Chem. Soc.* **1996**, *118*, 3108.
- (8) Auffinger, P.; Hays, F.; Westhof, E.; Ho, P. *Proc. Natl. Acad. Sci. U. S. A.* **2004**, *101*, 16789.
- (9) Politzer, P.; Lane, P.; Concha, M.; Ma, Y.; Murray, J. J. *Mol. Model.* **2007**, *13*, 305.
- (10) Riley, K.; Hobza, P. *J. Chem. Theory Comput.* **2008**, *4*, 232.
- (11) Alkorta, I.; Rozas, I.; Elguero, J. *J. Phys. Chem. A* **1998**, *102*, 9278.
- (12) Cambi, R.; Cappelletti, D.; Liuti, G.; Pirani, F. *J. Chem. Phys.* **1991**, *95*, 1852.
- (13) Cappelletti, D.; Liuti, G.; Pirani, F. *Chem. Phys. Lett.* **1991**, *183*, 297.
- (14) Aquilanti, V.; Cappelletti, D.; Pirani, F. *Chem. Phys.* **1996**, *209*, 299.
- (15) Hobza, P.; Havlas, Z. *Chem. Rev.* **2000**, *100*, 4253.
- (16) Wang, W.; P., H. *J. Phys. Chem.* **2008**, *112*, 4114.
- (17) Zhao, Q.; Feng, D.; Hao, J.; Cai, Z. *J. Mol. Struct.* **2010**, *958*, 71.
- (18) Bernal-Uruchurtux, M.; Kerenskaya, G.; Janda, K. *Int. Rev. Phys. Chem.* **2009**, *28*, 223.
- (19) Cooke, S.; Cotti, G.; Evans, C.; Holloway, J.; Kisiel, Z.; Legon, A.; Thumwood, A. *Chem.—Eur. J.* **2001**, *7*, 2295.
- (20) Valerio, G.; Raos, G.; Meille, S.; Metrangolo, P.; Resnati, G. *J. Phys. Chem. A* **2000**, *104*, 1617.
- (21) Zou, J. W.; Jiang, Y.-J.; Guo, M.; Hu, G.-X.; Zhang, B.; Liu, H. C.; Yu, Q. *S. Chem.—Eur. J.* **2005**, *11*, 740.
- (22) Brammer, L.; Bruton, E.; Sherwood, P. *Cryst. Growth Des.* **2001**, *1*, 277.
- (23) Metrangolo, P.; Resnati, G. *Science* **2008**, *321*, 918.
- (24) Voth, A.; Khuu, P.; Oishi, K.; Ho, P. *Nat. Chem.* **2009**, *1*, 74.
- (25) Laguna, A.; Lasanta, T.; Lopez-de Luzuriaga, J.; Monge, M.; Naumov, P.; Olmos, M. E. *J. Am. Chem. Soc.* **2010**, *132*, 456.
- (26) Belpassi, L.; Tarantelli, F.; Pirani, F.; Candori, P.; Cappelletti, D. *Phys. Chem. Chem. Phys.* **2009**, *11*, 9970.
- (27) Rocaratti, L.; Belpassi, D.; Cappelletti, Pirani, F.; Tarantelli, F. *J. Phys. Chem. A* **2009**, *113*, 15223.
- (28) Belpassi, L.; Reca, M.; Tarantelli, F.; Roncaratti, L.-F.; Pirani, F.; Cappelletti, D.; Faure, A.; Scribano, Y. *J. Am. Chem. Soc.* **2010**, *37*, 132.
- (29) Pirani, F.; Candori, P.; Pedrose Mundim, M.; Belpassi, L.; Tarantelli, F.; Cappelletti, D. *Chem. Phys.*, in press, (2011), DOI: 10.1016/j.chemphys.2011.03.030.
- (30) Legon, A. *Angew. Chem., Int. Ed.* **1999**, *38*, 2686.
- (31) Caminati, W.; Maris, A.; Dell'Erba, A.; Favaro, P. *Angew. Chem., Int. Ed.* **2006**, *45*, 6711.
- (32) Mierzwicki, K.; Mielke, Z.; Saldyka, M.; Coussan, S.; Roubin, P. *Phys. Chem. Chem. Phys.* **2008**, *10*, 1292.
- (33) Torii, H. *Chem. Phys. Lett.* **2004**, *393*, 153.
- (34) Cappelletti, D.; Candori, P.; Rocaratti, L.; Pirani, F. *Mol. Phys.* **2010**, *108*, 2179.
- (35) Pirani, F.; Maciel, G. S.; Cappelletti, D.; Aquilanti, V. *Int. Rev. Phys. Chem.* **2006**, *25*, 165.
- (36) Cappelletti, D.; Bartolomei, M.; Pirani, F.; Aquilanti, V. *J. Phys. Chem. A* **2002**, *106*, 10764.
- (37) Pirani, F.; Cappelletti, D.; Vecchiocattivi, F.; Vattuone, L.; Gerbi, A.; Rocca, M.; Valbusa, U. *Rev. Sci. Instrum.* **2005**, *75*, 349.
- (38) Aquilanti, V.; Cappelletti, D.; Pirani, F.; Roncaratti, L. F. *Int. J. Mass Spectrom.* **2009**, *280*, 72.
- (39) Pirani, F.; Vecchiocattivi, F.; van den Biesen, J. J. H.; van den Meijdenberg, C. J. N. *J. Chem. Phys.* **1981**, *75*, 1042.
- (40) Aquilanti, V.; Ascenzi, D.; Cappelletti, D.; de Castro, M.; Pirani, F. *J. Chem. Phys.* **1998**, *109*, 3898.
- (41) Cappelletti, D.; Aquilanti, V.; Cornicchi, E.; Moix-Teixidor, M.; Pirani, F. *J. Chem. Phys.* **2005**, *106*, 024302.
- (42) Pirani, F.; Brizi, S.; Roncaratti, L. F.; Casavecchia, P.; Cappelletti, D.; Vecchiocattivi, F. *Phys. Chem. Chem. Phys.* **2008**, *10*, 5489.
- (43) Dunning, T. H. *J. Chem. Phys.* **1989**, *90*, 1007.
- (44) Woon, D. E.; Dunning, T. H. *J. Chem. Phys.* **1994**, *100*, 2975.
- (45) Woon, D. E.; Dunning, T. H. *J. Chem. Phys.* **1993**, *98*, 1358.
- (46) Werner, H.-J.; Knowles, P. J.; Lindh, R.; Manby, F. R.; Schütz, M. et al. *MOLPRO, A Package of ab Initio Programs*, version 2008.1, <http://www.molpro.net>.
- (47) Hodges, M. P.; Wheatley, R. J.; Schenter, G. K.; Harvey, A. H. *J. Chem. Phys.* **2004**, *120*, 710–720.
- (48) Boys, S. F.; Bernardi, F. *Mol. Phys.* **1970**, *19*, 553–566.